Inorg. Chem. **2004**, *43*, 5044–5052

Probing the Limits of the Zintl Concept: Structure and Bonding in Rare-Earth and Alkaline-Earth Zinc-Antimonides $Yb_9Zn_{4+x}Sb_9$ and $Ca_9Zn_{4.5}Sb_9$

Svilen Bobev*

Los Alamos National Laboratory, LANSCE-12/MS H805, Los Alamos, New Mexico 87545

Joe D. Thompson and John L. Sarrao

Los Alamos National Laboratory, MST-10/MS K764, Los Alamos, New Mexico 87545

Marilyn M. Olmstead, Håkon Hope, and Susan M. Kauzlarich

Department of Chemistry, University of California, One Shields Avenue, Davis, California 95616

Received February 9, 2004

A new transition metal Zintl phase, $Yb_9Zn_{4+x}Sb_9$, was prepared by high-temperature flux syntheses as large single crystals, or by direct fusion of the corresponding elements in polycrystalline form. Its crystal structure was determined by single-crystal X-ray diffraction. Its Ca-counterpart, hitherto known as $Ca_9Zn_4Sb_9$, and the presence of nonstoichiometry in it were also studied. $Yb_9Zn_{4+x}Sb_9$ was found to exist in a narrow homogeneity range, as suggested from the crystallographic data at 90(3) K (orthorhombic, space group *Pbam* (No. 55), $Z = 2$): (1) $a = 21.677(2)$ Å, $b = 12.3223(10)$ Å, $c = 4.5259(4)$ Å, R1 = 3.09%, wR2 = 7.18% for $Yb_9Zn_{4.23(2)}Sb_9$; (2) $a = 21.706(2)$ Å, $b = 12.3381(13)$ Å, $c = 4.5297(5)$ Å, R1 = 2.98%, wR2 = 5.63% for $Yb_9Zn_{4.380(12)}Sb_9$; and (3) $a = 21.700(2)$ Å, $b = 12.3400(9)$ Å, $c = 4.5339(4)$ Å, R1 = 2.75%, wR2 = 5.65% for $Yb_9Zn_{4.384(14)}Sb_9$. The isostructural $Ca_9Zn_{4.478(8)}Sb_9$ has unit cell parameters $a = 21.830(2)$ Å, $b = 12.4476(9)$ Å, and $c = 4.5414(3)$ Å (R1 = 3.33%, wR2 = 5.83%). The structure type in which these compounds crystallize is related to the $Ca_9Mn_4Bi_9$ type, and can be considered an interstitially stabilized variant. Formal electron count suggests that the Yb or Ca cations are in the +2 oxidation state. This is supported by the virtually temperature-independent magnetization for $Yb_9Zn_{4.5}Sb_9$. Electrical resistivity data show that $Yb_9Zn_{4.5}Sb_9$ and $Ca_9Zn_{4.5}Sb_9$ are poor metals with room-temperature resistivity of 10.2 and 19.6 mΩ·cm, respectively.

Introduction

Polar intermetallic phases formed between the electropositive alkaline-earth (Ca, Sr, Ba) and divalent rare-earth metals (Eu, Yb) with the early post-transition elements from group 13 (Al, Ga, In) and the pnicogens, i.e., group 15 (P, As, Sb, Bi), have been the subject of increasing attention over the past two decades.[1–4] Systematic studies in recent years have revealed a large number of novel and peculiar structures, often with unusually complicated bonding patterns.[4–6] Regardless of this structural intricacy and diversity the Zintl concept, in many cases, has been successfully applied for rationalization of their structures and bonding. In highly abbreviated terms, the Zintl formalism assumes complete transfer of valence electrons from the electropositive elements to the electronegative ones, i.e., formally reducing them.[7] Hence, the electropositive atoms can be viewed simply as

* Author to whom correspondence should be addressed. E-mail: sbobev@lanl.gov.

(1) Schäfer, H.; Eisenmann, B.; Müller, W. *Angew. Chem., Int. Ed. Engl.* **1973**, *12*, 694.
(2) (a) von Schnering, H.-G. *Angew. Chem., Int. Ed. Engl.* **1981**, *20*, 33. (b) Schäfer, H. *Annu. Rev. Mater. Sci.* **1985**, *15*, 1.
(3) Eisenmann, B.; Cordier, G. In *Chemistry, Structure, and Bonding of Zintl Phases and Ions*; Kauzlarich, S. M., Ed.; VCH Publishers: New York, 1996; p 61.
(4) (a) Corbett, J. D. *Struct. Bonding* **1997**, *87*, 157. (b) Corbett, J. D. *Angew. Chem., Int. Ed.* **2000**, *39*, 670. (c) Corbett, J. D. In *Chemistry, Structure, and Bonding of Zintl Phases and Ions*; Kauzlarich, S. M., Ed.; VCH Publishers: New York, 1996; p 139.

10.1021/ic049836j CCC: $27.50
Published on Web 07/16/2004

spectator cations, while the electronegative atoms rearrange to form partial anionic sub-lattices with varying degrees of localized and/or delocalized bonding. This is done in such a way that the classic octet (8-N) rule is satisfied and closed-shell electronic configurations are achieved.[1−7]

The introduction of electronegative transition metal elements (TM), such as Zn, Cd, Mn, etc., to the subject of Zintl chemistry brings additional inherent complexity to the electronic structure that can be used as a tool with almost unlimited potential for discovering interesting magnetic and electronic properties in these systems. For example, just one family of Zintl compounds, the series $AE_{14}(TM)Pn_{11}$ and $RE_{14}(TM)Pn_{11}$ (AE = Ca, Sr, Ba; RE = Eu, Yb; TM = Zn, Cd, Mn; Pn = P, As, Sb, Bi), offers a wide range of properties, spanning semiconducting behavior, large or colossal magnetoresistance, ferro-magnetism, mixed-valency, nonstoichimetry, etc.[5] This combination of complex electrical, structural, and thermal properties might also have promise in the growing area of molecule-based magnets where the solid-state structures consist of arrays of molecular units similar to typical Zintl phases.[8]

The uniqueness of these compounds at the metal−insulator boundary and their relationship to other correlated electron systems have motivated us to undertake more thorough studies of other ternary systems, specifically zinc- and manganese-containing antimonides. Herein, we report the synthesis and the structural characterization of a new transition metal Zintl phase, $Yb_9Zn_{4+x}Sb_9$. Its orthorhombic structure (space group *Pbam* (No. 55), $Z = 2$) was found to exist in a narrow homogeneity range, i.e., $Yb_9Zn_{4+x}Sb_9$ ($0.2 < x < 0.5$), as suggested from the single crystal and powder X-ray data. The structure is closely related to the structure of the recently reported $Yb_9Zn_4Bi_9$,[9] a compound suggested to be a mixed-valent Yb analogue of $Ca_9Zn_4Bi_9$.[10] Notably, the entire family of $AE_9(TM)_4Pn_9$ phases (AE = Ca, Sr; TM = Zn, Cd, Mn; Pn = Sb, Bi) are reportedly fully stoichiometric, yet electron-deficient compounds.[10] This ambiguity provided motivation for reexamination of the archetype "$Ca_9Zn_4Sb_9$",[10] the reported structure of which was found to be inaccurate. The correct structure of $Ca_9Zn_{4.5}Sb_9$ and its physical properties are reported concurrently with the ones for the new Zintl phase $Yb_9Zn_{4+x}Sb_9$ (for simplicity $Yb_9Zn_{4.5}Sb_9$ hereafter).

Experimental Section

Synthesis. All manipulations were performed under vacuum or in an inert atmosphere. The starting materials (pure elements) were used as received. Yb (pieces, Ames 99.9%, or dendritic, Alfa 99.9%), Ca (granules, Alfa 98.8%), Zn (shot, Alfa, 99.999%), Sb (ingot, Alfa 99.99%), Sb_2O_3 (powder, Alfa 99.6%), and ZnO (powder, Alfa 99.99%) were loaded in new alumina crucibles, which were then put into fused silica ampules. The ampules were in turn closed under vacuum (or high purity Ar at 1/5 atm) by flame sealing. No reaction between the reactants and Al_2O_3 was observed. The atomic ratio of Yb/Zn/Sb = 9:4:9 was used in this reaction, which was carried out in an alumina crucible at 1000 °C for 4 h only, and then quickly brought to 800 °C. After a week at that temperature, the mixture was allowed to slowly cool to room temperature at a rate of −3 °C/hour.

$Yb_9Zn_{4.5}Sb_9$ was initially identified as one of the products of a reaction loaded as $Yb_{14}Zn_xSb_{11}$ ($x > 50$), which was intended to produce large single crystals of the mixed-valent $Yb_{14}ZnSb_{11}$ from a molten Zn solution.[5f] The reaction mixture was heated in a programmable muffle furnace using the following temperature profile: quick ramping (150 °C/hour) to 875 °C, dwell (below the bp of the solvent) for 1 week, followed by a slow cooling (−3 °C/hour) to 475 °C. At that point, the molten Zn was removed by centrifugation. Reactions with In and/or Sn as a flux, carried out in a similar manner, also proved successful. Details on flux-growth synthetic procedures can be found elsewhere.[11] Some reactions were investigated using Sb_2O_3 and/or ZnO as additional reagents, following the procedure for alumina crucibles described above using the stoichiometric ratio: 9:4:0.5:9 (Yb/Zn/O/Sb). In addition, reactions using the stoichiometry 9:4:9 (Yb/Zn/Sb) were set up in Ta tubes, and precautions were made to avoid possible contamination during the glovebox and/or arc-welder operations.[5] The welded tubes were then jacketed in evacuated fused-silica ampules and treated with similar temperature profiles. Attempts were made to also synthesize $Ca_9Zn_4Sb_9O_{0.5}$ from a reaction mixture containing CaO and ZnO, in either alumina crucibles or sealed Ta tubes.

After the structure and the composition had been established from X-ray diffraction work, the synthesis of $Yb_9Zn_{4.5}Sb_9$ and $Ca_9Zn_{4.5}Sb_9$ was effectively reproduced from pure elements, loaded in atomic ratios (9:4.5:9 (Yb or Ca/Zn/Sb). These reactions were carried out in Al_2O_3 crucibles or sealed Ta tubes, jacketed in evacuated fused-silica ampules. The mixtures were typically heated to 800−1000 °C and were slowly cooled to room temperature.

Powder X-ray Diffraction. X-ray powder diffraction patterns were used to monitor the reaction outcomes; they were taken at room temperature on a Scintag XDS 2000 powder diffractometer using monochromatized Cu Kα radiation. The data analysis was carried out employing the JADE 6.5 software package.[12] The diffraction patterns were compared with those calculated from the single-crystal structure data using Crystal Diffract 4.1.[13] The product from reactions with the atomic ratio 9:4:9 (Yb/Zn/Sb) in all cases contained traces of impurity phases $Yb_{11}Sb_{10}$, Yb_4Sb_3, and $YbZn_2Sb_2$,[14] typically below 10 wt % (est.). The product from reactions

(5) (a) Kauzlarich, S. M. In *Chemistry, Structure, and Bonding of Zintl Phases and Ions*; Kauzlarich, S. M., Ed.; VCH Publishers: New York, 1996; p 245. (b) Chan, J. Y.; Olmstead M. M.; Kauzlarich, S. M.; Webb, D. J. *Chem. Mater.* **1998**, *10*, 3583. (c) Chan, J. Y.; Wang, M. E.; Rehr, A.; Kauzlarich, S. M. *Chem. Mater.* **1997**, *9*, 2131. (d) Chan, J. Y.; Kauzlarich, S. M.; Klavins, P.; Shelton, R. N.; Webb, D. J. *Chem. Mater.* **1997**, *9*, 3132. (e) Chan, J. Y.; Kauzlarich, S. M.; Klavins, P.; Shelton, R. N.; Webb, D. *J. Phys. Rev.* **1998**, *B57*, 8103. (f) Fisher, I. R.; Bud'ko, S. L.; Song, C.; Canfield, P. C.; Ozawa, T. C.; Kauzlarich, S. M. *Phys. Rev. Lett.* **2000**, *85*, 1120. (g) Young, D. M.; Torardi, C. C.; Olmstead, M. M.; Kauzlarich, S. M. *Chem. Mater.* **1995**, *7*, 93. (h) Gallup, R. F.; Fong, C. Y.; Kauzlarich, S. M. *Inorg. Chem.* **1992**, *31*, 115.
(6) Nesper, R. *Angew. Chem., Int. Ed. Engl.* **1991**, *30*, 789.
(7) Zintl, E. *Angew. Chem.* **1939**, *52*, 1.
(8) (a) Holmes, S. M.; Girolami, G. S. *J. Am. Chem. Soc.* **1999**, *121*, 5593. (b) Miller, J. S.; Epstein, A. J. *Chem. Eng. News* **1995**, *73*, 30.
(9) Kim, S.-J.; Salvador, J.; Bilc, D.; Mahanti, S. D.; Kanatzidis, M. G. *J. Am. Chem. Soc.* **2001**, *123*, 12704.
(10) (a) Brechtel, E.; Cordier, G.; Schäfer, H. *Z. Naturforsch.* **1979**, *34B*, 1229. (b) Brechtel, E.; Cordier, G.; Schäfer, H. *Z. Naturforsch.* **1981**, *36B*, 1099.
(11) Canfield, P. C.; Fisk, Z. *Philos. Mag. B* **1992**, *65*, 1117.
(12) JADE Version 6.5; Materials Data, Inc.: Livermore, CA, 2003.
(13) CrystalDiffract Version 4.1; CrystalMaker Software: Bicester, Oxfordshire, U.K., 2003.
(14) *Pearson's Handbook of Crystallographic Data for Intermetallic Phases*; Villars, P., Calvert, L. D., Eds.; ASM International: Materials Park, OH, 1991.

Table 1. Selected Crystallographic Data for $Yb_9Zn_{4.5}Sb_9$ and $Ca_9Zn_{4.5}Sb_9$

	1	2	3	4
chemical formula	$Yb_9Zn_{4.23(2)}Sb_9$	$Yb_9Zn_{4.380(12)}Sb_9$	$Yb_9Zn_{4.384(14)}Sb_9$	$Ca_9Zn_{4.478(8)}Sb_9$
fw	2929.54	2939.60	2939.61	1749.38
space group, Z		*Pbam* (No. 55), 2		
unit cell parameters	$a = 21.677(2)$ Å	$a = 21.706(2)$ Å	$a = 21.700(2)$ Å	$a = 21.830(2)$ Å
	$b = 12.3223(10)$ Å	$b = 12.3381(13)$ Å	$b = 12.3400(9)$ Å	$b = 12.4476(9)$ Å
	$c = 4.5259(4)$ Å	$c = 4.5297(5)$ Å	$c = 4.5339(4)$ Å	$c = 4.5414(3)$ Å
	$V = 1208.9(2)$ Å^3	$V = 1213.1(2)$ Å^3	$V = 1214.1(2)$ Å^3	$V = 1234.1(2)$ Å^3
radiation, λ (Å)		Mo Kα, 0.71073		
temperature, T (K)		90(3)		
ρ_{calcd} (g/cm^3)	8.048	8.048	8.042	4.708
μ (cm^{-1})	483.49	483.30	482.95	157.91
final R1 ($I > 2\sigma_I$)[a]	3.09%	2.98%	2.75%	3.33%
final wR2 ($I > 2\sigma_I$)[b]	7.18%	5.63%	5.65%	5.83%

[a] $R1 = \sum||F_0| - |F_c||/\sum|F_0|$. [b] $wR2 = [\sum[w(F_0^2 - F_c^2)^2]/\sum[w(F_0^2)^2]]^{1/2}$, and $w = 1/[\sigma^2F_0^2 + (AP)^2 + BP]$, $P = (F_0^2 + 2F_c^2)/3$; A and B are weight coefficients.

with the atomic ratio 9:4.5:9 (Yb or Ca/Zn/Sb) produced a powder diffraction pattern that could be fully indexed as $Yb_9Zn_{4.5}Sb_9$ or $Ca_9Zn_{4.5}Sb_9$. Powder patterns of crushed crystals of $Yb_9Zn_{4.5}Sb_9$ and $Ca_9Zn_{4.5}Sb_9$, before and after exposure to air and moisture for a period of more than three months, showed no differences in line intensities or positions, although the metallic luster of the crystals progressively diminished during that time. The measured lattice constants for various samples, synthesized under different conditions, with or without flux, showed small systematic differences; these are corroborated by the lattice parameters obtained from low-temperature single-crystal data (Table 1).

Single-Crystal X-ray Diffraction. Structure determination for $Yb_9Zn_{4.5}Sb_9$ was performed on three crystals from different reactions to exclude the possibility of impurity elements and to ascertain the potential phase width.

Additionally, structure determination for $Ca_9Zn_{4.5}Sb_9$ was performed with the idea to establish the uniqueness of $Yb_9Zn_{4.5}Sb_9$. Single crystals from different reactions were selected and cut under Exxon Paratone N oil to the desired dimensions. Then, the crystals were mounted on glass fibers and placed under a cold nitrogen stream (ca. −180 °C) on a Bruker SMART 1000 CCD diffractometer equipped with a CRYO COOLER low-temperature apparatus (CRYO Industries of America, Inc.). Hemispheres of data were collected for four crystals with graphite monochromatized Mo Kα radiation (ω-scans, $2\theta_{max}$ ~63°), Table 1. Three crystals of $Yb_9Zn_{4.5}Sb_9$ were chosen from different reactions (**1**−**3**) and one crystal for $Ca_9Zn_{4.5}Sb_9$ (**4**). **1** was selected from an alumina crucible reaction with the elements in a ratio of Yb/Zn/Sb = 9:4:9 and carried out at 1000 °C (0.09 × 0.06 × 0.05 mm, dark-metallic, irregularly shaped; $T_{min}/T_{max} = 0.1047/0.1959$, 10672 total reflections, 2135 unique reflections, $R_{int} = 4.91\%$). **2** was selected from a Ta tube reaction of the elements in a ratio of Yb/Zn/Sb = 9:4:9 and carried out at 1000 °C (0.16 × 0.15 × 0.12 mm, dark-metallic, irregularly shaped; $T_{min}/T_{max} = 0.0480/0.0683$, 10569 total reflections, 2169 unique reflections, $R_{int} = 5.71\%$). **3** was selected from a Zn flux reaction heated at 875 °C (0.08 × 0.05 × 0.04 mm, dark-metallic, irregularly shaped; $T_{min}/T_{max} = 0.1225/0.2200$, 11064 total reflections, 2167 unique reflections, $R_{int} = 4.56\%$). **4** was selected from an alumina crucible reaction of the elements in a ratio of Ca/Zn/Sb = 9:4:9, carried out at 1000 °C (0.08 × 0.06 × 0.04 mm, dark-metallic, irregularly shaped; $T_{min}/T_{max} = 0.3653/0.5712$, 11188 total reflections, 2224 unique reflections, $R_{int} = 6.32\%$). Details of data collection are provided in Table 1.

The unit cell parameters for $Yb_9Zn_{4.5}Sb_9$ ($a \approx 21.7$, $b \approx 12.3$, $c \approx 4.5$ Å), especially the very short c axis, were confirmed by taking long-exposure axial pictures. The systematic absence conditions $k = 2n + 1$ for $0kl$ and $h = 2n + 1$ for $h0l$ suggested only two possible space groups—the noncentrosymmetric *Pba*2 (No. 32) and the centrosymmetric *Pbam* (No. 55). The latter was chosen based on intensity statistics calculations and relevant figures of merit. The structure of $Yb_9Zn_{4.5}Sb_9$ (Figure 1) was subsequently solved by direct methods and refined to convergence. The data were corrected for Lorentz and polarization effects and integrated in Laue symmetry *mmm* using the SMART and SAINT software.[15] Multiscan absorption correction was applied with the use of the SADABS software package.[16] Data were subsequently refined on F^2 (data-to-parameter ratio greater than 27) with the SHELXTL V5.10 package.[17] All atoms were refined with anisotropic displacement parameters with scattering factors and absorption coefficients from the International Tables for Crystallography, Volume C.[18]

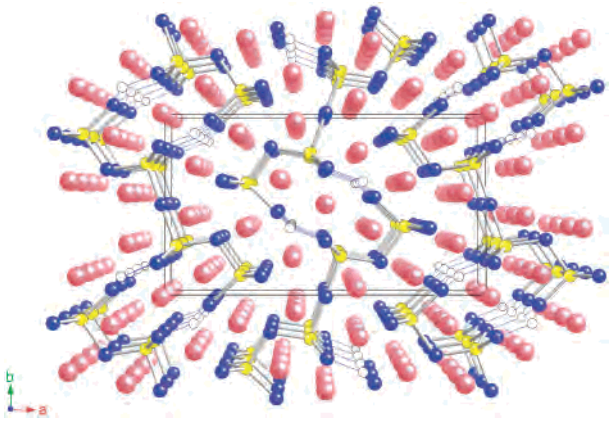

Figure 1. Perspective ball-and-stick representation of the orthorhombic structure of $Yb_9Zn_{4.5}Sb_9$ viewed along the c axis (unit cell is outlined). The Yb atoms are shown as large red spheres, the Sb atoms are shown as small dark blue spheres. The Zn atoms that center the $ZnSb_4$ tetrahedra (Zn1 and Zn2) are drawn as small yellow spheres, and the interstitial Zn atoms (Zn3) are drawn as empty circles.

Positional and equivalent isotropic displacement parameters and important bond distances for $Yb_9Zn_{4.380(12)}Sb_9$ and $Ca_9Zn_{4.478(8)}Sb_9$ are listed in Tables 2 and 3, respectively. During the first least-squares cycles, all atoms were refined with isotropic atomic displacement parameters (U's hereafter). The refinement following

(15) (a) SMART NT Version 5.05; Bruker Analytical X-ray Systems, Inc.: Madison, WI, 1998. (b) SAINT NT Version 6.22; Bruker Analytical X-ray Systems, Inc.: Madison, WI, 2001.
(16) SADABS NT Version 2.05; Bruker Analytical X-ray Systems, Inc.: Madison, WI, 1998.
(17) SHELXTL Version 5.10; Bruker Analytical X-ray Systems, Inc.: Madison, WI, 1997.
(18) *International Tables for Crystallography, Volume C*, 6th ed.; Wilson, A. J. C., Prince, E., Eds.; Kluwer Academic Publishers: Norwell, MA, 1999; p 548.

Table 2. Atomic Coordinates and Equivalent Isotropic Displacement Parameters (U_{eq}[a]) for $Yb_9Zn_{4.5}Sb_9$ and $Ca_9Zn_{4.5}Sb_9$

atom	site	*x*	*y*	*z*	U_{eq} (Å^2)
		$Yb_9Zn_{4.380(12)}Sb_9$			
Sb1	2*d*	0	1/2	1/2	0.0056(2)
Sb2	4*g*	0.4964(1)	0.3069(1)	0	0.0071(2)
Sb3	4*g*	0.3061(1)	0.1204(1)	0	0.0066(2)
Sb4	4*h*	0.3527(1)	0.4585(1)	1/2	0.0056(2)
Sb5	4*h*	0.1680(1)	0.3090(1)	1/2	0.0050(2)
Yb1	2*b*	0	0	1/2	0.0076(2)
Yb2	4*g*	0.1387(1)	0.1349(1)	0	0.0072(1)
Yb3	4*g*	0.0907(1)	0.4351(1)	0	0.0062(1)
Yb4	4*g*	0.2620(1)	0.3763(1)	0	0.0081(1)
Yb5	4*h*	0.3987(1)	0.2093(1)	1/2	0.0087(1)
Zn1	4*h*	0.0464(1)	0.2759(1)	1/2	0.0083(3)
Zn2	4*h*	0.2395(1)	0.1172(1)	1/2	0.0086(3)
Zn3[b]	4*g*	0.3957(4)	0.3922(8)	0	0.021(3)
		$Ca_9Zn_{4.478(8)}Sb_9$			
Sb1	2*d*	0	1/2	1/2	0.0055(2)
Sb2	4*g*	0.4966(1)	0.3060(1)	0	0.0070(1)
Sb3	4*g*	0.3051(1)	0.1227(1)	0	0.0070(1)
Sb4	4*h*	0.3524(1)	0.4597(1)	1/2	0.0051(2)
Sb5	4*h*	0.1668(1)	0.3094(1)	1/2	0.0048(2)
Ca1	2*b*	0	0	1/2	0.0096(5)
Ca2	4*g*	0.1379(1)	0.1366(1)	0	0.0092(4)
Ca3	4*g*	0.0914(1)	0.4396(1)	0	0.0070(3)
Ca4	4*g*	0.2608(1)	0.3779(1)	0	0.0091(3)
Ca5	4*h*	0.3974(1)	0.2109(1)	1/2	0.0115(4)
Zn1	4*h*	0.0455(1)	0.2791(1)	1/2	0.0085(2)
Zn2	4*h*	0.2388(1)	0.1202(1)	1/2	0.0091(2)
Zn3[b]	4*g*	0.3967(2)	0.3945(4)	0	0.017(2)

[a] U_{eq} is defined as $^1/_3$ of the trace of the orthogonalized U_{ij} tensor. [b] Interstitial Zn site, partially occupied with refined occupancy of: (**1**) 11.3(8)% for $Yb_9Zn_{4.23(2)}Sb_9$; (**2**) 19.0(6)% for $Yb_9Zn_{4.380(12)}Sb_9$; (**3**) 19.2(7)% for $Yb_9Zn_{4.384(14)}Sb_9$; and (**4**) 23.9(4)% for $Ca_9Zn_{4.478(8)}Sb_9$.

only 6 least-squares cycles converged at excellent R1 and wR2 factors, 4.50 and 11.95%, respectively, and all atoms had quite reasonable *U*'s. However, there was a residual peak of approximately 18 e$^-$/Å^{-3} ~2.5 Å from Sb2. The peak remained essentially unchanged after refinement with anisotropic *U*'s. Aluminum, oxygen, carbon, and nitrogen were also investigated as possible elements, but were discarded for lack of a suitable fit. The peak was interpreted as the result of a partially occupied Zn site. Refining the added Zn site (Zn3) with fractional occupancy and isotropic *U* resulted in improvement of R1 from 3.69 to 3.03%. The highest peak in the final difference map was of nearly the same magnitude as the deepest hole, approximately 2.7 e$^-$/Å^3. The site occupancy factor for Zn3 (Table 2) was close to 20%, far from 100%. The full occupancies for all other atoms (five Yb, five Sb, and two Zn) were verified by refining their site occupancy factors. Except for Zn3, all occupancies refined to within 5σ of 100%. The final refinement of the structure was done with occupancies for the regular atoms fixed at 100%, and a variable occupancy for Zn3 (Table 2). The refinement converged at R1 and wR2 factors of 2.98 and 5.63%, respectively. The final difference map revealed virtually no unaccounted-for density. The largest excursions (about ±3 e$^-$/Å^{-3}) were associated with Yb2.

Magnetic Susceptibility Measurements. Magnetization field cooling measurements were performed in a Quantum Design MPMS SQUID magnetometer from 2 to 350 K in a magnetic field of 0.1 T. Several samples from different reactions were measured to establish the reproducibility of the results. In all cases the phase purity was verified by powder X-ray diffraction. The samples, with a typical weight of approximately 20 mg, were loaded in plastic straws and secured between two small pieces of quartz wool. The raw data were corrected for the holder's diamagnetic contribution and converted to molar susceptibility. To determine the Yb formal oxidation state, molar susceptibility was normalized per mole of Yb.

Resistivity Measurements. The electrical resistivity measurements were carried out on a Quantum Design PPMS system from 5 to 300 K using a four-probe technique. The applied AC current of 1 mA had a frequency of 15.9 Hz. Resistance as a function of temperature for both $Yb_9Zn_{4.5}Sb_9$ and $Ca_9Zn_{4.5}Sb_9$ was measured on a variety of samples to ensure reproducibility. For the data reported herein, polished single crystals of **3** and **4** were used.

Elemental Analysis. Single crystals of $Yb_9Zn_{4.5}Sb_9$ were obtained from several different reactions and were mounted onto carbon tape. The samples were then placed in a Cameca SX100 electron microscope equipped with a wavelength-dispersive spectrometer. The microprobe was operated at 15 nA beam current at 20 keV accelerating potential. In the backscattering electron and reflected images some surface oxidation could be clearly seen, however, enough smooth and impurity-free surfaces were still present and were used for the analysis. Potential oxygen, carbon, and aluminum inclusions were of particular interest, but there was no evidence of elements other than Yb, Zn, and Sb. Pure elements were used as standards, which precluded the precise determination of the Yb-content due to a partial surface degradation of the standard, and resulted in a somewhat broad range of totals—from 97.8(9)% to 102.6(9)%. Nonetheless, the relative amounts of Zn and Sb were determined precisely; the resulting ratio of Sb/Zn = 2.04(1) was established based on 15 spots (1-μm diameter, 30-s counting time) from two different crystals of $Yb_9Zn_{4.380(12)}Sb_9$. This agrees very well with the Sb/Zn ratio of 2.05 obtained from single-crystal X-ray data (Table 1).

Results and Discussion

Synthesis. Small, dark, brittle crystals with metallic luster were originally isolated from a Zn flux reaction and used in the initial structural studies by means of powder and single-crystal X-ray diffraction (below). The product appears to be quite stable based on powder X-ray diffraction. However, the surfaces slowly lose their reflectivity over a period of about 3 months, suggesting the formation of a passivating oxide layer. This oxide surface did not appear to change the diffraction intensities and therefore must be extremely small. Initially, the structure was presumed to be $Yb_9Zn_4Sb_9$, and reaction was set up to obtain the compound in high yield. Several temperature profiles were explored; in all cases powder X-ray diffraction indicated that the product contained traces of impurity phases. No reaction conditions could be found, using the ratio 9:4:9 (Yb/Zn/Sb), to produce 100% yield of the desired product. This fact, together with the problems encountered during the refinement of the single-crystal data, prompted us to investigate the possibility of an oxygen-stabilized phase. Examples of interstitial derivatives such as La_5Pb_3O are well-known among polar intermetallics.[19] For that purpose, a few mixtures of the elements were loaded with Sb_2O_3 and/or ZnO as additional reactants. The products from these reactions showed a mixture of phases—oxides, unreacted elements, some Yb−Zn and Zn−Sb binaries, and only trace amounts of the desired $Yb_9Zn_4Sb_9$ compound. All investigations indicated that oxygen was not a possible interstitial in the product.

(19) Guloy, A.; Corbett, J. D. *Z. Anorg. Allg. Chem.* **1992**, *616*, 61.

Table 3. Important Bond Distances (Å) in $Yb_9Zn_{4.5}Sb_9$ and $Ca_9Zn_{4.5}Sb_9$

$Yb_9Zn_{4.38012)}Sb_9$						$Ca_9Zn_{4.478(8)}Sb_9$					
Sb1−	2 × Zn1	2.942(2)	Yb1−	2 × Sb4	3.2388(8)	Sb1−	2 × Zn1	2.924(1)	Ca1−	2 × Sb4	3.2612(6)
	4 × Yb3	3.1065(4)		4 × Sb2	3.2882(6)		4 × Ca3	3.115(1)		4 × Sb2	3.3157(4)
	2 × Yb5	3.3921(6)		4 × Zn3	3.467(7)		2 × Ca5	3.451(2)		4 × Zn3	3.459(4)
Sb2−	Zn3	2.426(8)		2 × Zn1	3.550(2)	Sb2−	Zn3	2.441(4)		2 × Zn1	3.613(1)
	2 × Zn1	2.7115(9)	Yb2−	Zn3	3.086(9)		2 × Zn1	2.7234(7)	Ca2−	Zn3	3.108(6)
	Yb2	3.1703(9)		2 × Sb4	3.1467(7)		Ca2	3.168(2)		2 × Sb4	3.170(1)
	2 × Yb1	3.2882(6)		2 × Zn2	3.158(1)		2 × Ca1	3.3157(4)		2 × Zn2	3.169(1)
	2 × Yb5	3.3290(7)		Sb2	3.1703(9)		2 × Ca5	3.353(1)		Sb2	3.170(1)
	Yb3	3.621(1)		2 × Sb5	3.1852(7)		Ca3	3.692(2)		2 × Sb5	3.190(1)
Sb3−	2 × Zn2	2.6868(8)		2 × Zn1	3.488(1)	Sb3−	2 × Zn2	2.6939(6)		2 × Zn1	3.518(2)
	Yb3	3.2001(9)		Sb3	3.6388(9)		Ca3	3.208(2)		Sb3	3.654(2)
	2 × Yb5	3.2199(7)		Yb3	3.8468(8)		2 × Ca5	3.228(1)		Ca3	3.905(3)
	Yb4	3.299(1)		Yb4	3.8520(8)		Ca4	3.320(2)		Ca4	3.906(2)
	Yb4	3.355(1)		Yb4	4.0038(8)		Ca4	3.371(2)		Ca4	4.027(1)
	Yb2	3.6388(9)	Yb3−	2 × Sb1	3.1065(4)		Ca2	3.654(2)	Ca3−	2 × Sb1	3.115(1)
Sb4−	2 × Zn3	2.583(4)		2 × Zn1	3.148(1)	Sb4−	2 × Zn3	2.599(2)		2 × Zn1	3.187(1)
	Zn2	2.799(2)		Sb3	3.2001(9)		Zn2	2.820(1)		Sb3	3.208(2)
	2 × Yb2	3.1467(7)		2 × Sb5	3.2192(6)		2 × Ca2	3.170(1)		2 × Sb5	3.239(1)
	2 × Yb4	3.1677(6)		Sb2	3.621(1)		2 × Ca4	3.192(1)		Sb2	3.692(2)
	Yb5	3.234(1)		Yb4	3.7873(8)		Ca5	3.249(2)		Ca4	3.777(2)
	Yb1	3.2388(8)		Yb2	3.8468(8)		Ca1	3.2612(6)		Ca2	3.905(3)
Sb5−	Zn1	2.671(2)	Yb4−	Zn3	2.909(9)	Sb5−	Zn1	2.675(1)	Ca4−	Zn3	2.974(5)
	Zn2	2.831(2)		2 × Sb5	3.1592(6)		Zn2	2.830(1)		2 × Sb5	3.178(1)
	2 × Yb4	3.1592(6)		2 × Sb4	3.1677(6)		2 × Ca4	3.178(1)		2 × Sb4	3.192(1)
	2 × Yb2	3.1852(7)		Sb3	3.299(1)		2 × Ca2	3.190(1)		Sb3	3.320(2)
	2 × Yb3	3.2192(6)		Sb3	3.355(1)		2 × Ca3	3.239(1)		Sb3	3.371(2)
Zn1−	Sb5	2.671(2)		2 × Zn2	3.737(1)	Zn1−	Sb5	2.675(1)		2 × Zn2	3.776(2)
	2 × Sb2	2.7115(9)		Yb3	3.7873(8)		2 × Sb2	2.7234(7)		Ca3	3.777(2)
	Sb1	2.942(2)		Yb2	3.8520(8)		Sb1	2.924(1)		Ca2	3.906(2)
Zn2−	2 × Sb3	2.6868(8)		Yb2	4.0038(8)	Zn2−	2 × Sb3	2.6939(6)		Ca2	4.027(1)
	Sb4	2.799(2)	Yb5−	2 × Zn3	3.198(7)		Sb4	2.820(1)	Ca5−	2 × Zn3	3.221(4)
	Sb5	2.831(2)		Zn1	3.212(1)		Sb5	2.830(1)		Zn1	3.234(2)
Zn3−	Sb2	2.426(8)		2 × Sb3	3.2199(7)	Zn3−	Sb2	2.441(4)		2 × Sb3	3.228(1)
	2 × Sb4	2.583(4)		Sb4	3.234(1)		2 × Sb4	2.599(2)		Sb4	3.249(2)
	Yb4	2.909(9)		2 × Sb2	3.3290(7)		Ca4	2.974(5)		2 × Sb2	3.353(1)
	Yb2	3.086(9)		Sb1	3.3921(6)		Ca2	3.108(6)		Sb1	3.451(2)
	2 × Yb5	3.198(7)		Zn2	3.636(1)		2 × Ca5	3.221(4)		Zn2	3.642(2)

To eliminate the possibility for Al as an impurity (possibly from the Al_2O_3 crucibles), tantalum tubes were used as the reaction vessel. The product was investigated by single-crystal X-ray diffraction and the refinements of the data were inconsistent with the reported "9−4−9" structure type, as there was a peak of significant height (approximately 12−19 $e^-/Å^3$) remaining in the difference electron density map (below).

To determine unequivocally the nature of this additional and previously unreported electron density, several reactions were set up with Ca in place of Yb. Calcium is an element with much lower *Z*-number and a Ca−Zn−Sb compound has been already reported with the 9−4−9 structure type.[10] Hence, mixtures of pure Ca, Zn, and Sb were loaded and treated exactly the same way as the Yb-reactions. Both flux growth and direct fusion techniques, both in alumina crucibles and sealed Ta tubes, were employed. Oxygen was also explored similarly to the Yb phase, and those reactions proved unsuccessful in producing the 9−4−9 compound in high yield.

The reactions in alumina crucibles and tantalum tubes, with the atomic ratio 9:4.5:9 (Yb or Ca/Zn/Sb) produced the desired phase in quantitative yield. Some Zn might be lost due to evaporation. $Yb_9Zn_{4.5}Sb_9$ was the only product from the Zn flux. The results from the reactions investigated, along with the microprobe data, provided strong evidence for the previously overlooked interstitial to be Zn.

Structure Determination. Intensity data were collected for several crystals, aimed at unambiguous determination of the structure and to ascertain its potential phase width for both $Yb_9Zn_{4.5}Sb_9$ and $Ca_9Zn_{4.5}Sb_9$. Table 1 provides details on all four data collections and refinement parameters.

All four structures reported here have excess electron density at positions corresponding to the partially occupied Zn3, but with different occupancies, depending on the method of preparation. This consistency provides further support that the additional Zn is a real feature of the structures and not an artifact.

The structure was determined to be of a new type, which can be regarded as an interstitially stabilized variant of the $Ca_9Mn_4Bi_9$ structure type (Pearson's code *oP*44; space group *Pbam*, $a = 22.42(2)$ Å; $b = 12.56(1)$ Å; $c = 4.72(1)$ Å; $Z = 2$).[10] To better illustrate the differences between this "Zn-stuffed" derivative and the parent 9−4−9 structure (Figure 2) the unit cell axes and the nomenclature for the atomic positions were assigned accordingly.

During the first least-squares cycles, it became immediately obvious that there was a residual peak of approximately 18 $e^-/Å^{-3}$ ~2.5 Å from Sb2 (Figure 2). The persistence and size of the peak led us to conclude that it was a property of the structure, rather than a result of absorption effects. It was interpreted as the result of a partially occupied Zn site. The choice of Zn was confirmed by microprobe analysis and by exploring a variety of synthetic conditions (Experimental Section).

To determine whether the Yb-compound is unique, the structure of $Ca_9Zn_4Sb_9$ was reexamined and its physical properties were measured (below). These studies were

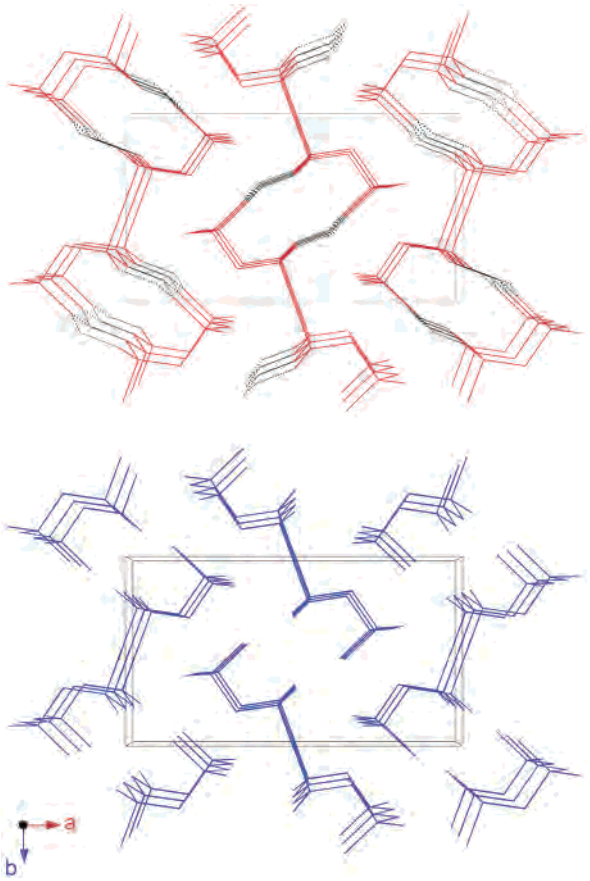

Figure 2. Wire-frame representation of the two-dimensional $[Zn_{4.5}Sb_9]^{18-}$ anionic sublattice in $Yb_9Zn_{4.5}Sb_9$ (red), compared with the one-dimensional $[Zn_4Sb_9]^{19-}$ ribbon-like chains (blue) in the imaginary $Yb_9Zn_4Sb_9$. The Yb cations are omitted for clarity.

performed with crystals produced from the reaction of the pure elements carried out at conditions similar to those described in the original report.[10] In this instance, the substitution of Yb with Ca, a much lighter element, resulted in excellent single-crystal X-ray data, and the subsequent structure determination for $Ca_9Zn_{4.478(8)}Sb_9$ presents unequivocal evidence that the compound requires an interstitial Zn. Tables 2 and 3 provide positional parameters and bond distances for $Yb_9Zn_{4.380(12)}Sb_9$ and $Ca_9Zn_{4.478(8)}Sb_9$.

Structure Description. The main structural features in the new structure type are fragments of four corner-shared tetrahedral units of $ZnSb_4$, running parallel to the *c*-axis as shown in Figure 3. These are further interconnected through an extra atom and *exo*-bonds to form a channel-like two-dimensional structure, with Yb^{2+} or Ca^{2+} cations occupying the empty space within and between the channels (Figure 1). Similar structural motifs and packing arrangements are known in the 9−4−9 structure, which is originally described as one-dimensional "ribbonlike" chains (Figure 2), with cations separating them.[9,10]

Two crystallographically unique Zn-sites (Zn1 and Zn2) and five crystallographically unique Sb-sites are common for both the parent 9−4−9 structure and its interstitially stabilized derivative (Table 2). These seven positions account for the two pairs of zinc-centered $ZnSb_4$-tetrahedra with shared corners, which are related to each other by *b*- and

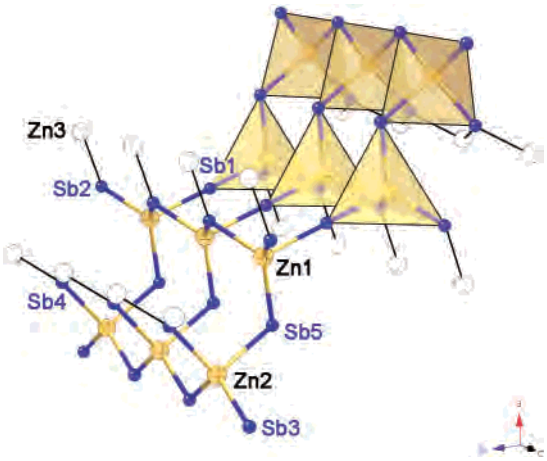

Figure 3. Detailed view of a segment of the two-dimensional $[Zn_{4.5}Sb_9]^{18-}$ anionic sub-lattice in both $Yb_9Zn_{4.5}Sb_9$ and $Ca_9Zn_{4.5}Sb_9$. Emphasized is the way the Zn-centered $ZnSb_4$ tetrahedra share corners to form the "ribbonlike" one-dimensional chains—building units in the "9−4−9" structure. The interstitial Zn-atoms, Zn3, bridge these chains through *exo*-bonds into a two-dimensional channel-like structure.

a-glides (Figure 3). As a result of that, one of the five Sb atoms, Sb1 (Wyckoff site 2*d* with 2/*m* symmetry, Table 2), is located at the center of the four-membered fragment (Figure 3). This rather unusual linear coordination accounts for the significant elongation of the corresponding Zn−Sb bonds (Table 3). For instance, in both $Yb_9Zn_{4.5}Sb_9$ and $Ca_9Zn_{4.5}Sb_9$, the resultant Zn1−Sb1 distances are considerably longer than the rest, 2.942(2) Å and 2.924(1) Å, respectively, which are almost 6% greater than the sum of the corresponding atomic radii of Zn and Sb.[20] Such linear environment is not comparable with any other antimonides. Only the central Pn-atom in linear Pn_3^{7-} polyanions found in the $AE_{14}(M)Pn_{11}$ and $RE_{14}(M)Pn_{11}$ families of compounds (AE = Ca, Sr, Ba; M = Al, Ga, In, Zn, Mn; Pn = P, As, Sb, Bi) could be regarded as similarly coordinated.[5] The bonding in these linear Pn_3^{7-} polyanions however, is described as hypervalent 3-center-4-electron, isoelectronic with I_3^- anions,[5h] whereas in all previous reports on 9−4−9 structures, these interactions are considered normal 2-center-2-electron bonds.[9,10]

As a consequence of the unusual linear environment of Sb1, the neighboring Zn-atoms are slightly displaced from the ideal center of the $ZnSb_4$-tetrahedra (Figure 3). The corresponding tetrahedral angles deviate somewhat from the ideal value of 109.5°, from 101.10(5) to 116.95(3)° in $Yb_9Zn_{4.5}Sb_9$, and from 101.40(4) to 116.29(2)° in $Ca_9Zn_{4.5}Sb_9$, respectively. Nevertheless, the Zn−Sb distances, varying from 2.6868(8) to 2.799(2) Å in $Yb_9Zn_{4.5}Sb_9$, and from 2.675(1) to 2.820(1) Å in $Ca_9Zn_{4.5}Sb_9$, are normal for single Zn−Sb bonds (Table 3).[20] They compare very well with the observed Zn−Sb distances in other ternary Yb−Zn−Sb and Ca−Zn−Sn phases, such as $YbZn_2Sb_2$ and $CaZn_2Sb_2$,[21] with Zn−Sb distances in the order of 2.69 to 2.79 Å.

Figure 4 shows the coordination sphere of the partially

(20) Pauling, L. *The Nature of the Chemical Bond*; Cornell University Press: Ithaca, NY, 1960.
(21) (a) Klüfers, P.; Neumann, H.; Mewis, A.; Schuster, H.-U. *Z. Naturforsch.* **1980**, *35B*, 1317. (b) Mewis, A. *Z. Naturforsch.* **1978**, *33B*, 382.

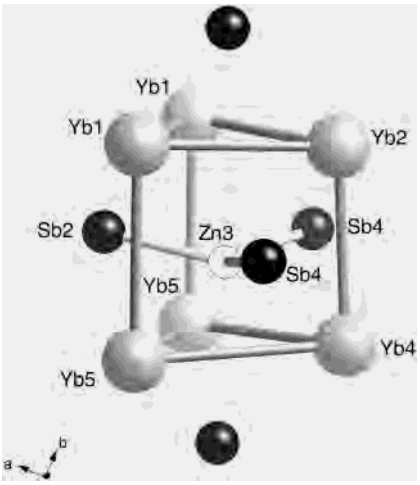

Figure 4. Local coordination of the interstitial Zn3 site. The corresponding bond distances are given in Table 3.

occupied Zn3 site. It does not resemble the tetrahedral coordination of the Zn1 and Zn2 sites. Zn3 has three next nearest Sb neighbors (Table 3); there are two other Sb's that are farther away at nonbonding distances. Zn3 occupies the empty center of a distorted trigonal prism formed by six Yb-atoms. All five faces of this Yb-based trigonal prism that hosts the interstitial Zn site are capped by the five Sb atoms.

The apparent Zn3−Sb2 and Zn3−Sb4 distances, varying from 2.426(8) to 2.583(4) Å, and from 2.442(4) to 2.599(2) Å, for $Yb_9Zn_{4.5}Sb_9$ and $Ca_9Zn_{4.5}Sb_9$, respectively, are too short for single Zn−Sb bonds.[20] They are clearly shorter than the rest. The most likely explanation for this is that the refined Sb positions are not representative of the real positions in the Zn3-occupied unit cells, as only 1 in 5 to 1 in 9 cells are occupied. The displacement ellipsoid for Sb2 clearly indicates a displacement of Sb2 along the Sb2−Zn3 vector. This will be the effect if a Zn3 occupation results in a shift of Sb2 in order to make room for Zn3.

The five crystallographically different Yb (or Ca) cations occupy the space between and within the channels (Figure 1) and have rather distinct coordination environments, as shown in Figure 5. The corresponding Yb−Sb, Yb−Zn, Ca−Sb, and Ca−Zn bond distances (Table 3) are very similar (Zn = Zn1 and Zn2, i.e., the tetrahedrally coordinated atoms). They all fall in the range from 3.1467(7) to 3.737(1) Å in $Yb_9Zn_{4.5}Sb_9$, and from 3.169(1) to 3.776(2) Å in $Ca_9Zn_{4.5}Sb_9$. The distances from the interstitial Zn3 site to Yb or Ca are shorter than the rest, at 2.909(9) and 3.467(7) Å in $Yb_9Zn_{4.5}Sb_9$, and 2.974(5) and 3.459(4) Å in $Ca_9Zn_{4.5}Sb_9$, respectively. Again, as in the case of the shorter Sb−Zn3 distances, the most likely explanation is that this is an artifact resulting from the low occupancy of Zn3. The Yb or Ca positions interact only with a small number of occupied Zn3 sites, so that the average distance that results from this model appears to be short. Otherwise, there are no close Yb−Yb or Ca−Ca interactions present in the structure—the shortest contacts are between Yb2−Yb3 (3.8468(8) Å) and between Yb3−Yb4 (3.7873(8) Å), and between Ca2−Ca3 (3.905(3) Å) and between Ca3−Ca4 (3.777(2) Å), respectively. None of the Yb or Ca sites is partially occupied, as already discussed in the previous section.

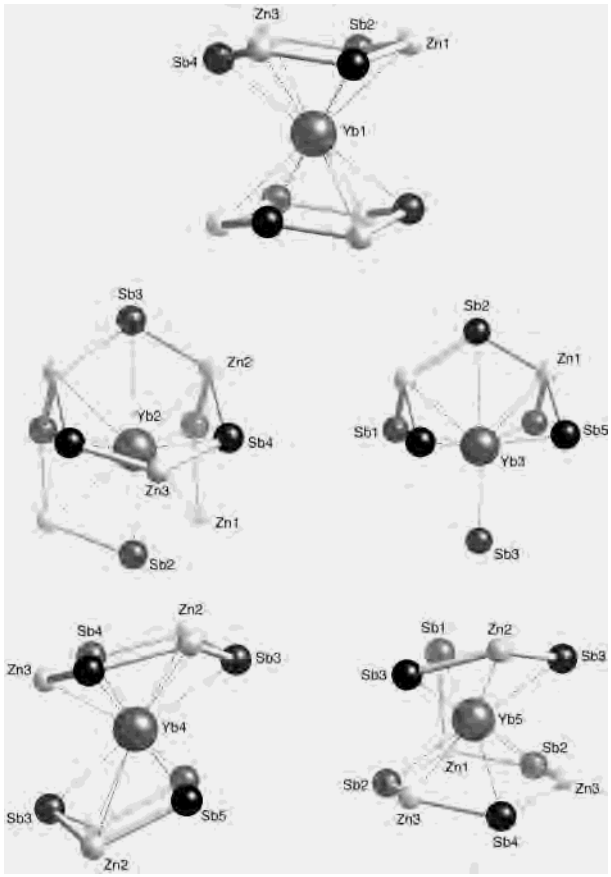

Figure 5. Next nearest neighbors of all five crystallographically independent Yb sites in $Yb_9Zn_{4.5}Sb_9$. Ca-coordination in $Ca_9Zn_{4.5}Sb_9$ is identical. The first coordination sphere cutoff has been set at 3.8 Å.

It should be noted here that the average Yb−Zn and Yb−Sb contacts in $Yb_9Zn_{4.5}Sb_9$ (excluding the shorter Zn3 distances) are 3.34, 3.28, 3.23, 3.22, and 3.32 Å, respectively. The corresponding averages of Ca−Zn and Ca−Sb contacts in $Ca_9Zn_{4.5}Sb_9$ (again excluding the shorter Zn3 distances) are 3.37, 3.29, 3.25, 3.24, and 3.34 Å. Evidently, in both structures Yb3 (or Ca3) and Yb4 (or Ca4) exhibit much stronger covalent interactions with the polyanionic sublattice, although their first coordination spheres do not differ much from the coordination spheres of the rest of the cations. Empirical bond-valence sum calculations support it, as evidenced by the greater positive charges on Yb3 and Yb4 reported for $Yb_9Zn_4Bi_9$.[9] If the interstitial Zn3 site with fractional occupancy is included in the bonding picture, the averages of Yb−Zn and Yb−Sb contacts in $Yb_9Zn_{4.5}Sb_9$ become 3.40, 3.27, 3.25, 3.20, and 3.28 Å, respectively. In $Ca_9Zn_{4.5}Sb_9$ the average distances follow the same trend because the partially occupied Zn3 site is at a much shorter distance to Yb4 (or Ca4) than to any other Yb- or Ca-atom (Table 3).

Properties. The physical properties measurements obtained on a number of samples with different synthetic methods are consistent with the presence of additional Zn compared with the "9−4−9" structure type. Magnetizations of different reaction batches of $Yb_9Zn_{4.5}Sb_9$ were measured to ensure reproducible results and typical data are plotted in Figure 6. In the temperature range 100−350 K the magnetic

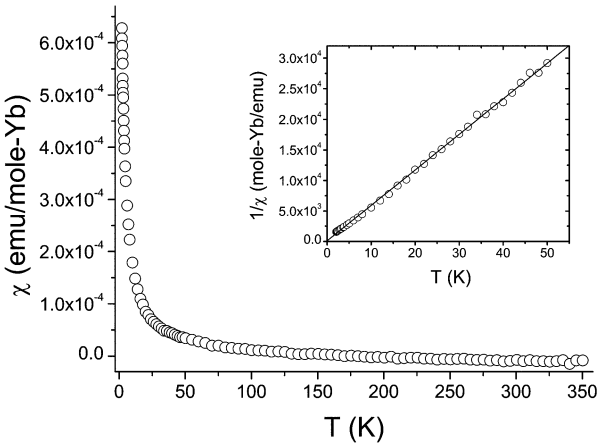

Figure 6. Temperature-dependent (2−350 K) magnetization data for $Yb_9Zn_{4.5}Sb_9$ measured at a field of 0.1 T. The inset shows the "impurity-contributed" paramagnetic regime for the inverse susceptibility $1/\chi(T)$.

susceptibility is nearly temperature-independent and weakly paramagnetic, as expected for divalent Yb (Figure 6).

Below ∼50 K, the inverse susceptibility $1/\chi(T)$ is nearly linear in temperature. In this paramagnetic regime, data could be fit to a modified Curie−Weiss model with Curie constant $C = 3.3 \times 10^{-3}$ emu·K·mol^{-1} and Weiss constant $\theta \approx -0.3$ K. Simple calculations give an effective moment of 0.16(2) μ_B/Yb, assuming that all Yb atoms contribute to the susceptibility. This effective moment is much smaller than the effective moment of 4.54 μ_B/Yb expected from Hund's rules for Yb^{3+} and larger than $\mu_{eff} = 0$ for Yb^{2+}.[22] A reasonable interpretation of these data is that Yb is divalent in $Yb_9Zn_{4.5}Sb_9$ and that there are small amounts of paramagnetic impurities in the sample. If the impurities were assumed to all be Yb^{3+}, an estimate of the volume fraction of Yb^{3+} in the sample can be made. With this assumption, the low-temperature susceptibility can be understood as arising from the presence of approximately 0.28% Yb^{3+}. These numbers indicate that in the $Yb_9Zn_{4.5}Sb_9$ structure all Yb cations are divalent.

Resistivity data were obtained for both flux-grown single crystals and polycrystalline samples to ensure reproducibility. Two representative plots of the electrical resistivity as a function of the temperature (5−300 K) for $Yb_9Zn_{4.5}Sb_9$ and $Ca_9Zn_{4.5}Sb_9$ are shown in Figure 7. The resistivity slowly decreases with decreasing temperature, suggesting metallic behavior. However, the large room-temperature values for both, 10.2 and 19.6 mΩ·cm, respectively, together with the small residual resistance ratios reveal semi- or rather poor metallic properties. This is consistent with the refined almost electron-precise compositions (Table 1), although Hall coefficient measurements are necessary to corroborate this hypothesis for low carrier concentration. Similar electrical resistivity properties are typical for many Yb-containing Zintl compounds, including examples of Yb mixed-valency in $Yb_9Zn_4Bi_9$ and $Yb_{14}ZnSb_{11}$.[9,5f]

Bonding and Electron Count. According to the Zintl formalism,[1−7] the electron count pertinent to the anionic sub-

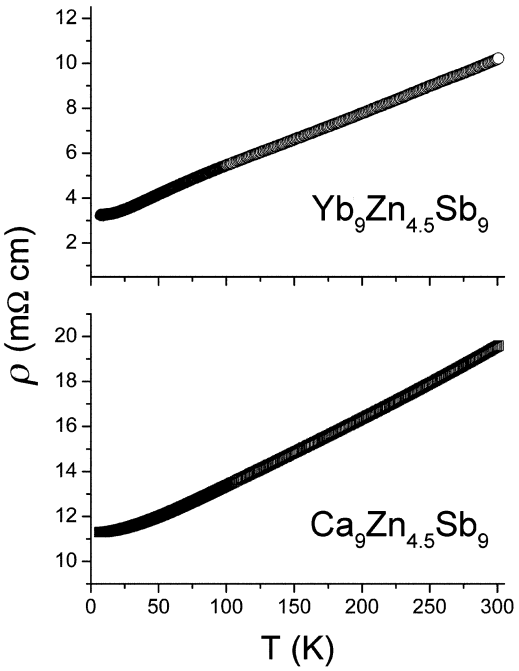

Figure 7. Temperature-dependent (5−300 K) resistivity data for $Yb_9Zn_{4.5}Sb_9$ and $Ca_9Zn_{4.5}Sb_9$ measured on flux-grown single crystals.

lattice of the 9−4−9 structure, can be described as $(4b\text{-}Zn^{2-})_4(1b\text{-}Sb^{2-})_2(2b\text{-}Sb^{1-})_7$, i.e., $[Zn_4Sb_9]^{19-}$.[9,10] Alternatively, one could rationalize the bonding strictly adhering to the valence rules as $4 \times (Zn^{2+}) + 9 \times (Sb^{3-}) = [Zn_4Sb_9]^{19-}$. Either scheme reveals a charge-imbalance because the electron count falls one electron short—there are only 9 divalent alkaline- or rare-earth counterbalancing cations, i.e., $9 \times 2 = 18$ positive charges, whereas the bonding in the anionic part as discussed above requires 19 electrons.

Following the discussion above, it is clear that the entire family of $AE_9(TM)_4Pn_9$ phases (AE = Ca, Sr; TM = Zn, Cd, Mn; Pn = Sb, Bi) poses challenging problems. It has been speculated that due to the presence of "nonclassical" structural features such as linear Zn1−Sb1−Zn1 motifs, along with possible partial covalent character in some bonds between alkaline-earth and pnicogens and/or the transition metals, the bonding may not be accurately explained in terms of the Zintl concept.[10] Instead, a new formulation as $[Zn_4Sb_9]^{x-}$ for the chains, where x is close to 18, is suggested.[9,10]

While the idea of variable electron count seems to work well for the alkaline-earth members of the 9−4−9 family of compounds, the report on the charge-balanced Zintl compound $Yb_9Zn_4Bi_9$ raises a question concerning the nature of the bonding across the series.[9,10] The interpretation of the published magnetic susceptibility data is that $Yb_9Zn_4Bi_9$ is a compound with mixed-valent Yb cations that obeys the classic Zintl rules. Thereby its electron count has been rationalized as $(Yb^{3+})(Yb^{2+})_8(Zn^{2-})_4(1b\text{-}Bi^{2-})_2(2b\text{-}Bi^{1-})_7$.[9] This suggests that the phase width for the Bi-analogue may be different from that found for the $Yb_9Zn_{4.5}Sb_9$. Since the compound is reported to be metallic, it is possible that the structure can exist without the additional Zn. However, further studies are necessary to explore this ambiguity.

(22) Smart, J. S. *Effective Field Theories of Magnetism*; Saunders: Philadelphia, PA, 1966.

Our systematic studies on the structure and properties of both $Yb_9Zn_{4.5}Sb_9$ and $Ca_9Zn_{4.5}Sb_9$ suggest that the originally determined 9−4−9 crystal structure is incorrect. The new structure type provides a better explanation for the electron count—now, according to the simple valence rules, the "9−4.5−9" composition yields a complete charge-balance, i.e., $9 \times (Yb^{2+}) + 4.5 \times (Zn^{2+}) = 9 \times (Ca^{2+}) + 4.5 \times (Zn^{2+}) = 9 \times (Sb^{3-})$.

Despite this apparent adherence to the classic octet (8-N) rule, both $Yb_9Zn_{4.5}Sb_9$ and $Ca_9Zn_{4.5}Sb_9$ systems are metallic (Figure 7), and it is not clear if the Zintl formalism truly holds. Similar effects in other Zn-containing Zintl phases are well-known, for example the whole subfamily of "14−1−11" phases $AE_{14}ZnSb_{11}$ and $AE_{14}CdSb_{11}$, where AE = Ca or Sr.[5g] These compounds invariably contain interstitial Sb's, however, and obey the Zintl rules only as nonstoichiometric $AE_{14}ZnSb_{11+x}$ and $AE_{14}CdSb_{11+x}$ phases.[5g] On the other hand, their Yb-analogue $Yb_{14}ZnSb_{11}$ is a line compound with no evidence of interstitials.[5f] The charge-balancing in this instance is clearly achieved through valence fluctuations.[5f]

As can be seen from the single-crystal X-ray data (Table 1), there are clear signatures of a narrow homogeneity range in $Yb_9Zn_{4.5}Sb_9$. The unit cell volume progressively increases as the refined concentration of the interstitial Zn increases too. On the basis of these numbers, it is possible to speculate that the compositions of $Yb_9Zn_{4.23(2)}Sb_9$ and $Yb_9Zn_{4.38(1)}Sb_9$ are the boundaries of the proposed homogeneity range—note that the first data are from a sample prepared in a stoichiometric manner in an Al_2O_3 crucible, i.e., some Zn might be lost due to evaporation, while the second dataset was collected for a crystal grown in Zn flux, i.e., an enormous excess of Zn.

On the basis of the above, $Yb_9Zn_{4.5}Sb_9$ appears to be able to accommodate wider ranges of interstitial Zn—the site occupancy for Zn3 varies from 11.3(8) to 19.2(7)% as shown in Table 2. Single-crystal X-ray diffraction work on crystals, selected from a reaction intended to produce $Ca_9Zn_4Sb_9$ (mixture of the elements in a ratio of 9:4:9, loaded in an Al_2O_3-crucible and heat-treated as reported originally),[10] provided strong evidence for the previously overlooked interstitial position, Zn3 (Table 2). The structure refinements suggest that the Zn3 site occupancy is 23.9(4)%, an indication of a virtually zero stoichiometry breadth. The unit cell volume of $Ca_9Zn_{4.5}Sb_9$, which is almost 20 Å^3 larger compared to the unit cell volume of $Yb_9Zn_{4.5}Sb_9$ (Table 1), although the effective ionic radii for Ca^{2+} and Yb^{2+} are virtually identical, 1.00 and 1.02 Å, respectively,[23] also agrees very well with the refined compositions of $Ca_9Zn_{4.478(8)}Sb_9$ and $Yb_9Zn_{4.384(14)}Sb_9$, respectively. These results seem to be in line with the observed room-temperature resistivities—ρ_{298} for the nearly charge-balanced Ca-compound is almost doubled relative to ρ_{298} of $Yb_9Zn_{4.5}Sb_9$, which deviates somewhat from the ideal electron count (Figure 7). The combination of poor metallic-like resistivity, large unit cell, and partial occupancy of the Zn3 site provides motivation for exploring the thermoelectric properties of these phases.

This more metallic behavior in $Yb_9Zn_{4.5}Sb_9$ of course could be due to many other factors, like Madelung energy, space filling, and possibly mixed valency. DFT band structure calculations for $Yb_9Zn_4Bi_9$ reveal substantial DOS near the Fermi level,[9] mainly composed of 4*f* bands of Yb and *p*-bands of Zn and Bi, indicating significant mixing. This points toward some degree of covalency in the Yb− interactions, which often seems to be ignored in similar intermetallic systems. In that sense it will be important to study in closer detail the band structure of $Yb_9Zn_{4.5}Sb_9$ and all other members of the 9−4−9 family. Such theoretical considerations supported by comprehensive and systematic structure−properties studies are currently under way.

Conclusions

We have synthesized and structurally characterized a new ternary transition metal polar intermetallic phase, $Yb_9Zn_{4.5}Sb_9$, which exists in a narrow homogeneity range. The structure of its Ca-analogue, $Ca_9Zn_{4.5}Sb_9$, and the presence of nonstoichiometry in it have also been studied. According to the presented data, nonstoichiometry is proposed as the most likely and obvious reason for the presumed electron deficiency in the whole $AE_9(TM)_4Pn_9$ family of compounds (AE = Ca, Sr; TM = Zn, Cd, Mn; Pn = Sb, Bi). This opens up the possibility to look into the crystal chemistry and the potential phase width for all these materials, as well as to reexamine their physical properties. Furthermore, since motivation for investigating new Zintl phases lies not only in their potential for offering new structure types and unique bonding arrangements, but also in their possible materials applications, especially as thermoelectrics, it will be worthwhile to explore the field for other possible transition metal analogues. This proves to be an essential approach to broadening our understanding of the chemistry and physics of polar intermetallic compounds, and to discover and tune useful properties in existing materials as well.

Acknowledgment. S.B. gratefully acknowledges the Laboratory-Directed Research and Development program (LANL-LDRD) for the Director's Postdoctoral Fellowship and the Institute for Complex Adaptive Matter (ICAM) for the financial support of this work. Work at LANL is done under the auspices of the U.S. DOE. S.M.K. acknowledges NSF for funding (DMR-0120990). We are indebted to Dr. V. Fritsch (LANL-MST) for her help with the four-probe measurements and Dr. S. Roeske (UC Davis) for assistance with the microprobe analysis.

Supporting Information Available: An X-ray crystallographic file (in CIF format) for the four structures. This material is available free of charge via the Internet at http://pubs.acs.org.

IC049836J

(23) (a) Shannon, R. D. *Acta Crystallogr.* **1976**, *A32*, 751. (b) Shannon, R. D.; Prewitt, C. T. *Acta Crystallogr.* **1969**, *B25*, 925.